Visible Light Induced Photodegradation of Methylene Blue (MB) Dye Over ZnO Modified α-Fe_2O_3 Nanocomposites

Abstract

The aim of this study was to synthesize Zinc (Zn) modified hematite (α-Fe_2O_3) nanocomposites with varying concentrations (pure, 10 wt%, 15 wt% and 20 wt%) via modified sol-gel method. The influence of dopant on structural, optical and photocatalytic activity of hematite were studied investigated.X-ray diffraction (XRD) pattern of synthesized samples was indexed to rhombohedral hematite with crystallite size ranging between 15–25 nm. Moreover, these materials were characterized by FTIR spectroscopy and scanning electron microscopy (SEM). The surface morphology of prepared nanoparticles was explored using scanning electron microscopy (SEM). The specific surface area of the solids was calculated from nitrogen adsorption isotherms by BET method. Photocatalytic properties of nanoparticles were performed for methylene blue (MB) dye and showed effective degradation in the presence of UV light. Hence, Zn^{2+} doped hematite can be considered as an efficient material for the potential applications in the domain of photocatalysis. Synthesized Zn doped hematite turned out to be superior degradation of MB dye in presence of UV-light.

Keywords: α-Fe_2O_3; Zn-doped α-Fe_2O_3; Nanocomposites; Photodegradation;

1. Introduction

Photocatalytic degradation of organic dyes in waste waters using metal oxide semiconductors has been considered as one of the most promising approaches to solving environmental pollution problems [1-5]. Significantly, metal oxide semiconductors (like TiO_2, ZnO, Nb_2O_5, WO_3, Fe_2O_3 etc.) have been demonstrated in photocatalytic application due to their potential characteristics, including high degradation efficiency, environment friendly, thermal stability, abundance, environment friendly, recyclable visible-light photocatalysis and low-cost products [6-12].

Ferrous oxide has four crystallographic phases, namely hematite (α-Fe_2O_3), maghemite (γ-Fe_2O_3), β-Fe_2O_3 and ε-Fe_2O_3. The thermodynamics stable hematite phase of Fe_2O_3 is a functional semiconductor with bandgap of 2.1 eV which is environmentally friendly, nontoxic and important in various field. Among them, hematite (α-Fe_2O_3) has been investigated extensively because they possess many attractive features, such as ease in handling, chemical stability, nontoxicity, an environment-friendly product, high resistance to corrosion features and the most stable iron oxide under ambient conditions [13-15]. The α-Fe_2O_3 can absorb visible light since it has a narrow bandgap ($E_g \approx$ 2.1 eV) compared to TiO_2, ZnO, WO_3 materials. Hematite is the widely investigated material due to its various applications in the field of photocatalyst, pigments, gas sensors, solar cells, electrochemical sensor and lithium-ion batteries etc. Since the structural and crystallographic forms are generally responsible for their properties, many methods for the synthesis of α-Fe_2O_3 including hydrothermal synthesis, forced hydrolysis , combustion method, microwave irradiation method, spray pyrolysis, chemical vapor deposition, pulsed laser deposition, co-precipitation and high vacuum

evaporation and sol-gel is mainly interesting method due to its low cost, high purity, short preparation time, homogeneous solution of doping element and magnify the excellent polycrystalline samples. By doping of different metal oxides, it will amplify to find new application and improve the performance of any other applications. Many researchers have focused on developing the mixed oxide semiconductors due to an efficient charge separation obtained by coupling two semiconductor particles with different energy levels [16-19].The improvement in efficiency of photocatalytic reactions is explained as result of a vectorial transfer of photo-generated electrons and holes from a semiconductor to another [20, 21]. In the present investigation, Zn doped hematite was synthesized by adopting modified sol-gel method. ZnO has electronic properties and band gap energy similar to that of TiO_2 and it has been reported sometimes to be more efficient than TiO_2 for the photooxidation of pollutants [22, 23].

Photocatalytic activity of a metal oxides depends on its preparation method since this affects the physicochemical properties of the solids. Sol-gel method is one of the most convenient methods for tailoring transition metal oxides to fit particular applications. The main advantage of the sol-gel method is the molecular level homogeneous mixing of transition-metal cation which enhances the formation of polycrystalline particles with special properties [24]. In this work, we reported the synthesis and characterization of mixed photocatalyst Zn doped α-Fe_2O_3 nanocomposites with varying concentrations (pure, 10 wt%, 15 wt% and 20 wt%) by modified sol-gel method. We studied the activity of the catalysts using as a test reaction the photocatalytic degradation of MB dye in aqueous dissolution.

2 Materials and Methods

2.1 Materials

All reagents used in the synthesis of Zn doped α-Fe_2O_3 nanoparticles used without any purification.$Fe(NO_3)_3.9H_2O$ and $Zn(NO_3)_2.6H_2O$ in a stoichiometry ratio was as precursor and diethylamine was used as a reagent and saturated solution of ammonia hydroxide was the precipitating agent, and double distilled water as solvent was used as a reaction medium.

2.2 Synthesis of pure and Zn doped α-Fe_2O_3 nanoparticles

The aqueous solution of appropriate amount of iron nitrate and zinc nitrate were dissolved in 100 ml of double distilled water. The mole ratio by wt% of dopant Zn and Fe was maintained as 10:90, 15:85 and 20:80. The mixture was allowed for magnetic stirring for 4 h. To this solution calculated quantity of diethylamine was added and stirring was continued for further 2 hr. Saturated solution of ammonium hydroxide was added and the mixture was allowed to stir for 2 h at 75°C. The brown-colored solution obtained was filtered and washed several times with water and ethanol. Then it was dried at 350°C in oven. The formed gel was calcined at 450 and 500°Cfor 3 hr.

2.3 Characterization

Synthesized nanocomposites were characterized by various spectroscopic techniques including, XRD, FTIR (Fourier Transform Infra-Red Spectrophotometry), SEM, UV-visible spectroscopy. By analyzing the N_2 adsorption-desorption isotherm and BJH utilizing a Micromeritics Analyzer (ASAP 2460) at 77 K, the surface area and pore size were estimated. A set of

photocatalytic degradation experiments of MB was carried out by photoreactor under UV light irradiation. The light source for photocatalysis was a visible light(40 W Hg lamp). The catalysts and solution were separated by filtration; the collected samples were analyzed by UV-Vis spectrophotometer (Shimadzu UV-2450). The photodegradation efficiency of RB5 has been calculated by applying the following equation:

$$\% \text{ Degradation efficiency} = \frac{C_o - C_t}{C_o} \times 100$$

Where,C_o is the original MB dye concentration, C_t is the retained MB dye concentration.

3. Result and discussion

3.1 X-ray diffraction

Analysis Structural and phase identification of the synthesized materials were confirmed using X-ray diffractionas shown in Figure 1. No diffraction peaks other than hematite has been observed, indicating that Zn atoms were incorporated inFe_2O_3 matrices. Thus, crystallinity is altered by dopant atoms without disturbing the rhombohedral structure of hematite. The crystal structure of the produced Zn doped hematitenanocomposites was determined and confirmed by using X-ray diffraction meter (Model Miniflex 600, RIGAKU, Japan) with Cu *kλ*radiation λ=1.5405 ´ over a wide range of Bragg angles. The crystalline size was calculated from the width of the XRD peaks, assuring that they are free from non-uniform strains. The particle size of the prepared samples was determined by using Scherer's equation [24] as follows –

$$D = \frac{0.95\lambda}{\beta cos\theta}$$

where λ is the X-ray wavelength, β is the full width at half maximum (FWHM) and θ is the diffraction angle, D is the average crystalline size perpendicular to the reflecting angle.

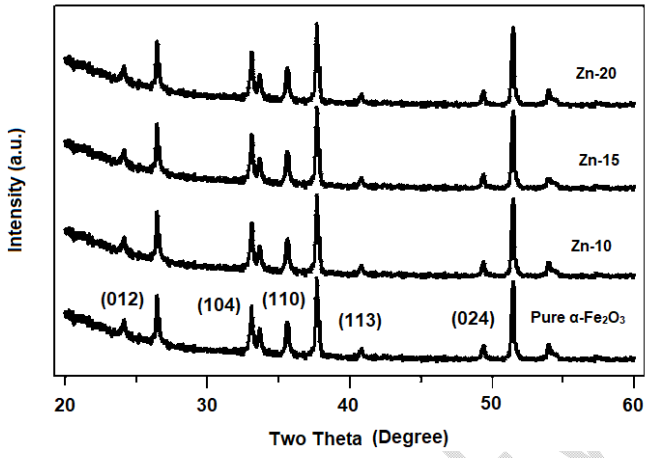

Figure 1. XRD pattern of pure and Zn doped α-Fe_2O_3materials.

The peaks at 2θ values of 24.27, 33.34, 35.80, 41.00, 49.64, 54.18, 62.66, and 64.17 correspond to the lattice planes (012), (104), (110), (113), (024), (116), (214) and (300) respectively. These planes represent the synthesized nanoparticles are in hematite phase, rhombohedral in structure. It's confirmed with JCPDS card No. 89-8104. The average crystallite size of nanoparticles obtained wereestimated using the Debye Scherer equation and was found to be 35 ± 20 nm.Itisalsonoticedthatasecondaryphasecorrespondingtothe(110)planeconfirmsthepresenceofZnintheFe2O3lattice. Whenthepercentageof zinc increasedto 15%,thecrystallinity ofthematerial falls furtherindicatingthatmorestrainis inducedintheFe2O3lattice.

3.2 Scanning electron microscopy (SEM)

Figure 2depicts the SEM micrographs of Zn dopedSEM micrographs exposed cluster appearances with crystalline natures. However, spherical structures of size ranging from 15-35 nm with irregular surface morphologies. The stony appearance might have been due to the aggregation of nanoparticles.

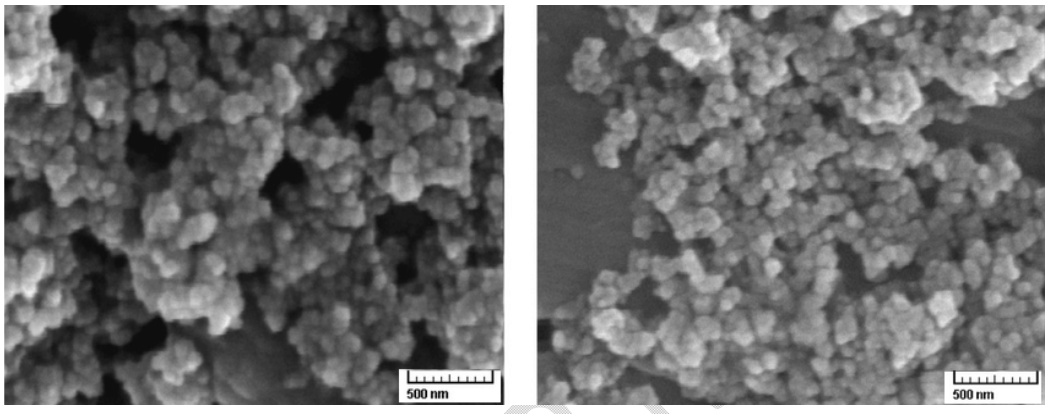

Figure 2 SEM images of sample.

3.3 FT-IR Studies

The presence of functional groups absorbed on the surface of synthesized pure and Zn-doped hematite nanocomposites wasdeterminedusingFT-IRspectroscopy.TheFT-IRspectraofpureZn-dopedhematitecalcinedat550°C are presented in Figure 3.As weseein Figure 3,thedistinctivebands are observed at3446,1642,571 and 478 cm^{-1}. The characteristic Fe-O two sharp peaks appear at 478 and 571 cm^{-1} and the broad band appear at 3446 cm^{-1} back to O-H of water molecules.In the region of 3430 cm^{-1} and 1639 cm^{-1}, the absorption band attributed to the stretching and bendingvibration of the water molecule is visible, and the bands of 568 cm^{-1} and 478 cm^{-1} are caused by the presence ofdopantandtheFe-Ovibrational

modeofhematitenanoparticles,whichareresponsibleforthe hematitephaseintherhombohedrallattice.

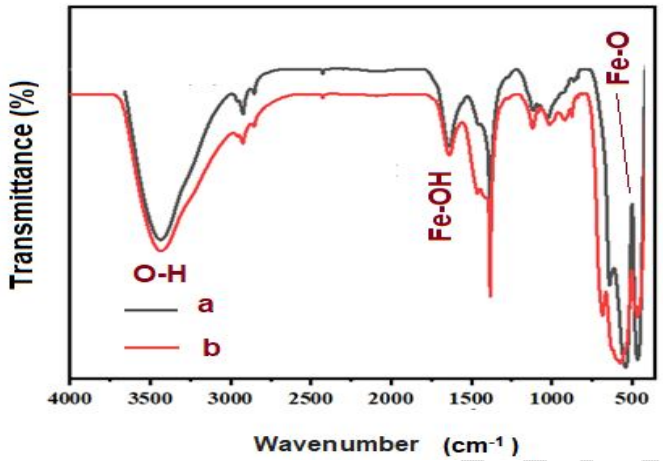

Figure 3 FT-IR spectra of (a) pure α-Fe_2O_3 and (b) Zn-15 sample.

3.4 UV-Vis absorption spectrum

The size of the particles plays an important role in changing the entire properties of nanomaterials. Therefore, size evolution of semiconducting nanoparticles becomes very essential to explore the properties of the materials. UV-visible absorption spectroscopy is widely being used technique to examine the optical properties of nanosized particles. The absorption spectrum of pure α-Fe_2O_3 and Zn-doped α-Fe_2O_3nanocomposites is shown in Figure 4. From Figure 5, one can see that the absorptionspectraintheUV–Visrangeofhematitesynthesizedexhibit an intenseabsorption intherange of 500–700nmwavelength.Thisresultis in good agreement withdata reported in otherstudies[5-7].Theopticalbandgap(E_g)forthe nanoparticlescanbedeterminedbyextrapolationfromtheabsorptionedgewhichisgivenbythefollowingequation:

$$(ahv)^n = A\,(hv - E_g)$$

Where α istheabsorptioncoefficient,*A*isconstant,*h*istheenergy oflightand*n*isaconstantdependingonthenatureoftheelectrontransition[].

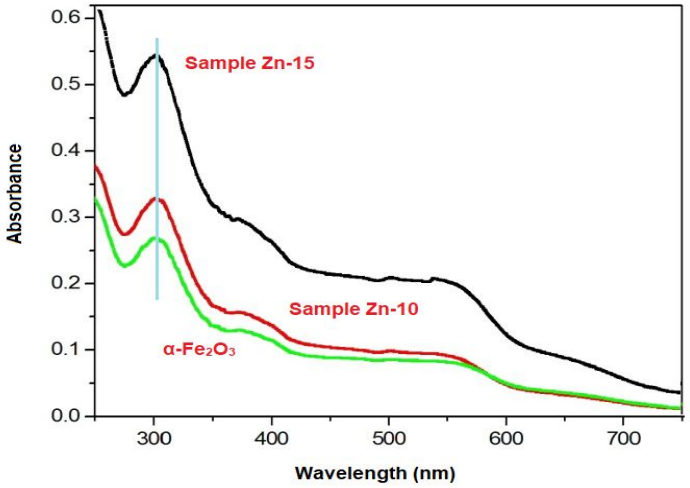

Figure 4 UV-Vis spectra of synthesized pure and Zn-doped Fe_2O_3 samples.

Table 1 Summary of BET-Specific Surface Area, Pore Volume, and Pore Size of the as synthesized samples.

Sample	BET specific surface area ($m^2\ g^{-1}$)	Pore volume (cm^3/g)	Pore size (A)
Pure α-Fe_2O_3	12.523	0.0121	29.2
Zn-10	16.569	0.0132	31.5
Zn-15	34.543	0.0456	42.2
Zn-20	17.459	0.0143	30.4

3.5 BET analysis

The surface area and porosity of the as synthesized nanomaterials were measured quantitatively using nitrogen adsorption BET. The samples were degassed at 150°C for 45 h before recording N_2 adsorption–desorption isotherms at −196°C. The BET surface area, pore volume and pore size of as synthesized samples are listed in Table 1. Noticeably, the surface area, pore volume, and pore size of Zn doped α-Fe_2O_3 materialsincreased compared to

pure α-Fe_2O_3. It is significant to mention that the photocatalytic performance is influenced by the surface area and size and volume; the higher the pore volume, porosity, and surface area, the higher the possibility for the catalyst to interact with and adsorb the pollutant.

3.6 Photocatalytic studies

Hematite is a semiconductor with a band-gap of 2.0–2.6 eV and can absorb from visible to UV region of the solar spectrum with assured wavelengths [27]. Therefore, synthesized nanomaterials can be used as a fine photocatalyst for speedy degradation of dyes. In this case, we evaluated the photocatalytic activities of as-prepared nanoparticles under UV-light irradiation using Methylene Blue (MB) aqueous solution as model contaminants. Methylene blue dye is solid at room temperature, odorless, and has a dark green powder color that changes to a blue color when dissolved in water. Methylene Blue (MB) is Phenothiazine dye that extensively used in dyeing, printing industries. It has severe toxic effects on the human health.According to the UV-visible research, MB has three absorption maxima (246nm, 291nm and 663nm). The absorption maxima wavelengths of MB (max) 291 and 663 nm) were widely employed for photodegradation of MB dye, respectively.The concentration of MB dye in the form of absorbance before and after photocatalytic degradation was measured at 663 nm (λ_{max} value obtained for Methylene Blue dye). In order to elucidate the effect of wt% of ZnO on the photocatalytic activity of α-Fe_2O_3photocatalyst, a set of parallel experiments were conducted with as synthesized photocatalysts containing different wt% of ZnO.The operating parameters such as effect of Zn doping, pH, catalyst

loading, initial dye concentration, effect of oxygen bubbling and effect of direct solar light on photodegradation of MB dye wasstudied.

The progress of the photocatalytic reaction was observed by taking absorbance at regular time intervals. It was observed that,hematite nanoparticles synthesized with higher dopant concentration tendtoyieldhigherremovalefficiencies.It was observed that the absorbance of MB dye decreased in presence of as-synthesized materials and UV-light as shown in Figure 5. The plot of absorbance versus time was linear. Hence, the reaction followed pseudo first order kinetics. The pseudo first order kinetic equationis presented below:

$$\ln \frac{C_O}{C_t} = kt$$

Where C_o and C_t are the concentrations of dye in solution at times 0 and t respectively, and k is the first-order rate constant (min^{-1}). It can be predicted from Figure 5, that after 100 minutes maximum degradation of MB dye was achieved for pure α-Fe_2O_3 sample.

3.6.1 Effect of Zn-doping

The photocatalytic capacity of Zn doped α-Fe_2O_3photocatalysts depends upon their ability to generate under irradiation ·OH radicals in aqueous solution. Moreover, ·OH radicals generation depends upon the dopant concentration in the host oxide. Figure 5shows thatwith increase in Zn concentration, degradation efficiency of MB dye increases with time and the bestdegradationefficiencycanbeachievedwithZn-15 in 72 min. This result suggests that Zn doped α-Fe_2O_3nanoparticles could be utilized as a good and

effective photo catalyst for removal of methylene blue as a pollutant from industrial effluent.

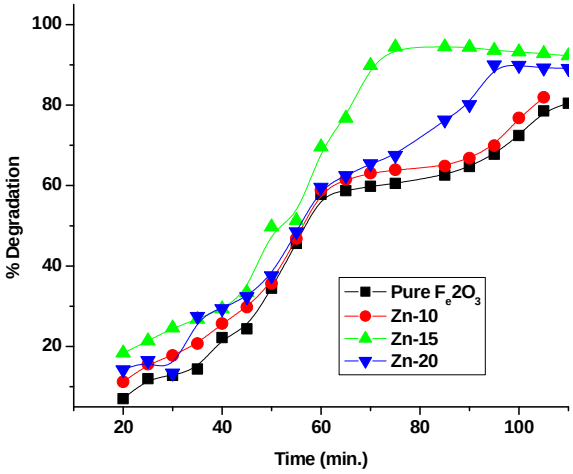

Figure 5 Photodegradation of MB dye using pure and doped α-hematite.

3.6.2 Effect of Catalyst dose

The effect of the dose of on the photodegradation of MB dye from the was observed. In the investigation, the dose of as synthesized pure and Zn doped α-Fe_2O_3nanocomposites was set to100-400 mg/L for initial dye concentration of 20 mg/L, at pH 2, irradiation source = UV-light. The observations are depicted in figure 5. It was observed that percent degradation increased with increase in catalyst dosage up to an optimum point. Further increase in catalyst dosage resulted in a decrease in the degradation of dye. The optimum dosage of catalyst was 200 mg/L. The initial increase in percent degradation could be attributed to the increase in the number of active sites on the catalyst surface as a result of increased catalyst dosage. With increase in the catalyst dosage, the number of free radicals viz., •OH and O_2^{2-} in solution are also increased consequently leading to enhanced photodegradation of the

wastewater sample [22].The decrease in the photodegradation later observed is attributed to the further increase in the catalyst dosage beyond the optimum, the suspended particles of the catalyst aggregate together and this reduces the amount of sunlight reaching the active sites of the catalyst and consequently, the rate of reaction decreases. This is also in agreement with the previous work [23-24].

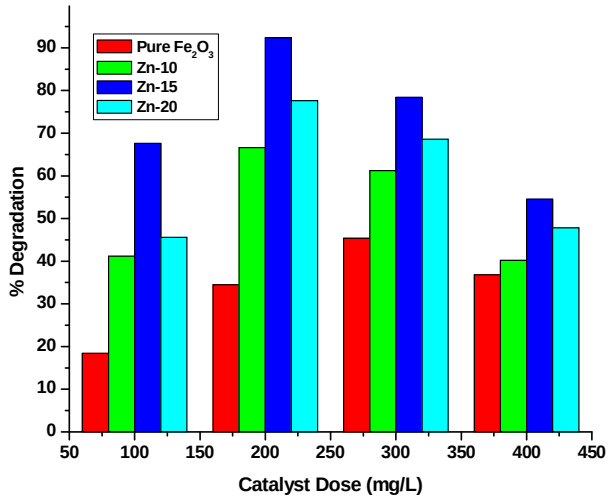

Figure 6Effect of catalyst dosage on MB dye degradation.

3.6.4 Effect of pH

pH in the photocatalytic study, controls the reactions during the degradation of dyes or organic compounds and beside this generation of hydroxyl radicals also depends on the pH of the solution [20, 21]. Initially the effect of pH on the photocatalytic degradation of MB dye in the range of pH 1–10 in presence of synthesized nanomaterials was studied under conditions (contact time = 120 min, dye concentration = 20 mg/L and catalyst dose = 1 g/L) as shown in Figure 7. The pH of a solution affects the surface charge

properties of the catalyst and indirectly it affects the adsorption behavior of the photocatalyst [22].

The percentage of dye removal showed an increase with decrease in pH value and reached their maximum value in the acidic region at pH 2. At low pH value, the surfaces of the catalysts were highly protonated and becomes positively charged so that the dye cations were electrostatically attracted more towards the catalyst surface as more oxidizing holes increases and thus degradation of MB dye was enhanced. At acidic pH, the positive holes are considered as the major oxidation species, whereas hydroxyl radicals are considered as the predominant species at neutral or alkaline pH [24]. Maximum degradation of MB dye at pH 2 for pure α-$Fe_2O_3$and Zn-15 sample was demonstrated 74.6% and 92.8% respectively.

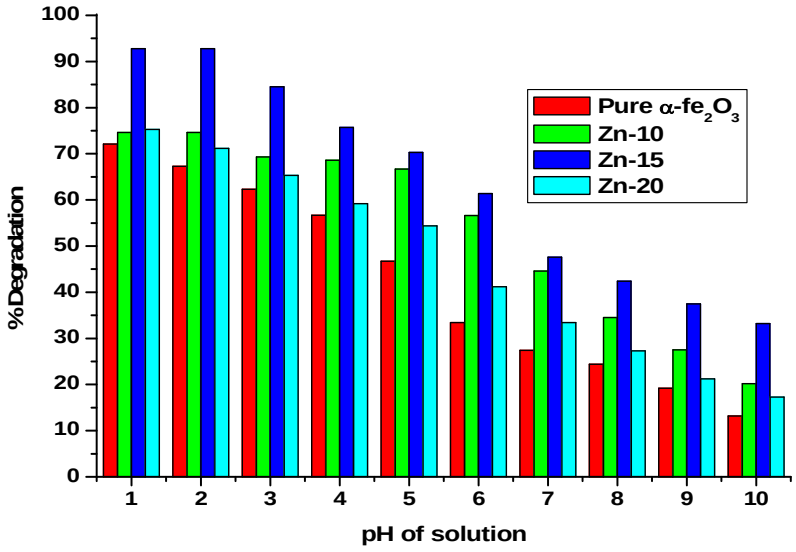

Figure 7Effect of pH on photodegradation of MB dye.

3.6.5 Effect of initial dye concentration

The effect of initial dye concentration on the degradation efficiency was studied at optimized pH = 2 with fixed catalyst dose by varying initial dye concentration. Different initial concentrations of MB dye with a range of 10–50 mg/L were used to assess the photocatalytic activity. Figure 8depicts the maximum dye degradation at the initial dye concentration of 20 mg/L. It was observed that, the degradation efficiency of dye was decreased when the initial concentration of dye increased. This is because; as the initial dye concentration was increased indirectly, the excess of dye molecules will be adsorbed on the catalyst surface, so the active sites of the catalysts will be reduced. As the dye concentration increases, a number of hydroxyl radicals are required for the degradation of dye molecules and while, the formation of hydroxyl radicals on the catalyst surface remains constant for given light intensity, catalyst dose and irradiation time [25]. Therefore, the hydroxyl radicals produced are insufficient for the degradation of dye at high concentration. Hence, photodegradation efficiency reduces as the concentration of dye increases.

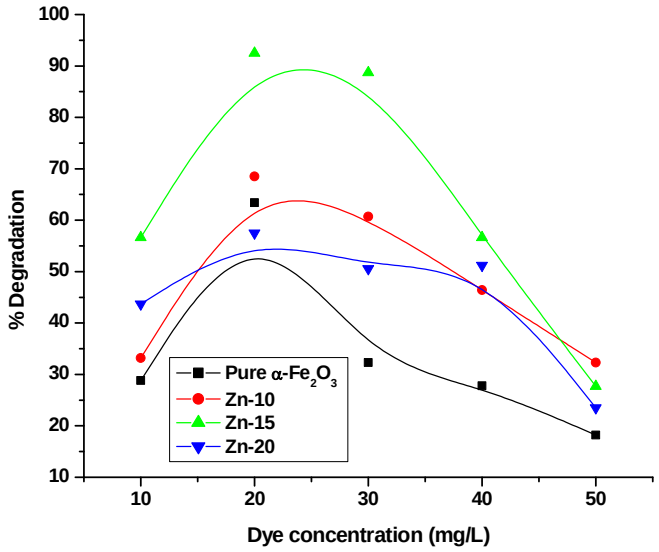

Figure8Effect of dye concentration on dye degradation at pH 2.

3.6.6 Effect of bubbling oxygen

In order to determine the influence of bubbling oxygen on the photocatalytic efficiency, MB dye degradation was performed by bubbling oxygen through an aqueous suspension containing 20 mg/L of dye and 1 g/L of Zn-15 catalyst. Moreover, photodegradation in deoxygenated medium was carried out after removal of oxygen by bubbling nitrogen for 30 min before closing the reactor by a septum to avoid any exchange with the external environment. The experimental observations are presented in Figure 9. It was noted that, the performance of degradation is higher in the oxygenated environment than in the non-oxygenated medium. Indeed, the yield of degradation of MB dye in the presence of oxygen is much larger (about 98.5%) than in the oxygen-free environment (about 92.4%).

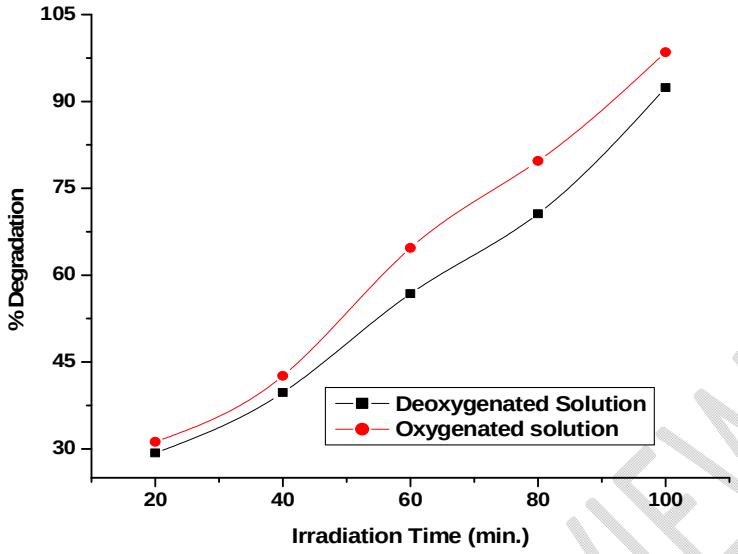

Figure 9Degradation of MB as a function of irradiation time in oxygenated and deoxygenated aqueous medium.

3.6.7 Solar light photodegradation of MB dye

Solar radiation has the advantage of being an inexhaustible energy emitted by the sun, a free source without any toxic effects on our environment. In addition, the two photocatalysts absorb a small percentage of the total sunlight intensity. It would be interesting to investigate the photocatalytic degradation of an aerated MB solution in the presence of the sample Zn-15 as presented in Figure 10. Experimentally, we followed the same experimental approach as UV irradiation; however, we exposed the MB dye (20 mg/L) solutions directly to the solar radiation(sunlight intensity at 355 nm). MB photodegradation under direct sunlight seems to be in progress after 55 min of solar light irradiation. In accordance with the significant sunlight intensity absorbed by the photocatalyst, the process of degradation was faster after 120 min.

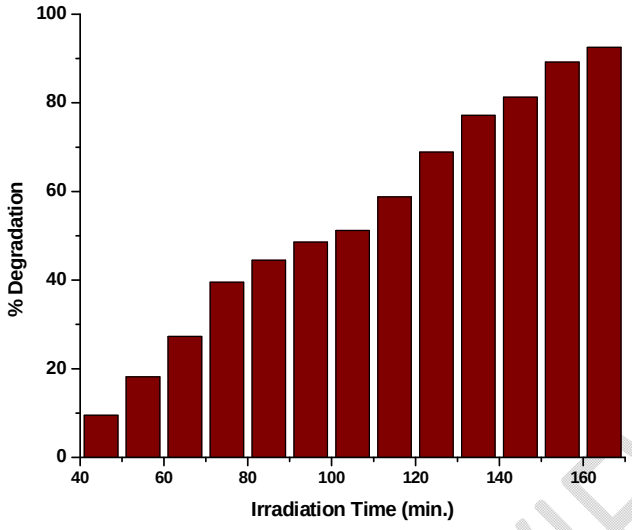

Figure 10Kinetics of the MB dye (20 mg/L) photocatalytic degradation using sample Zn-15 with solar light irradiation.

3.6.8 Reusability of photocatalyst

Presently. recovery and reusability are essential parameters for the selection of a cost-effective and feasible catalyst for pilot-scale remediation systems.

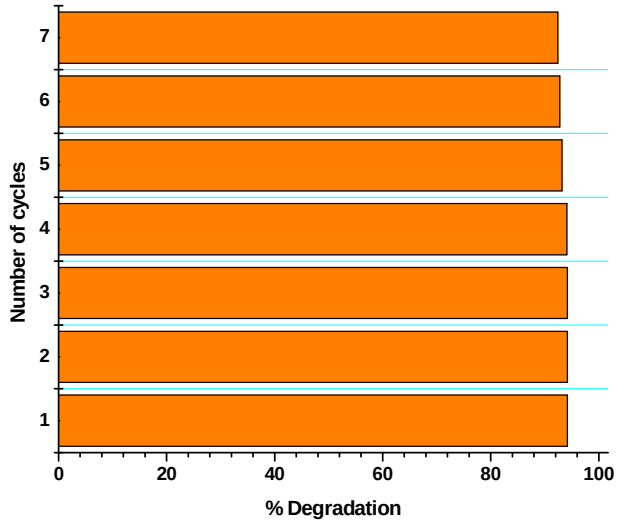

Figure 11Reusability function of Zn-15 sample for degradation of MB dye.

The reusability performance of the as synthesized nanomaterials was investigated for seven cycles of MB dye photodegradation using 100 mL of the MB dye (20 mg/L) at pH 2 with catalyst dose of 1 g/L. The recyclability and stability of the materialZn-15 after seven cycles during the 70min exposure is presented in Figure 11. The Zn-15 catalyst could be recycled conveniently after the treatment via a strong magnet and reused. After seven cycles, the photoactivity of Zn-15 catalyst decreased by 5% after seven successive cycles with high efficiency. This slight decrease in the photocatalysis activity could be attributed to the following: (i) Loss of materials occurred during washing and drying, which would lead to a lower dose in the subsequent cycle, thereby retarding the surface catalytic activity and degrading the performance [24]. (ii) The aggregation of nanoparticles can reduce the effective surface area and decrease the number of active sites and fouling, might change during the multiple cycles [35]. (iii) The adsorptive catalytic surface activity of the catalyst

gradually decreased because of the obstruction of the pores and the active sites by catechol and its intermediates after each cycle [36].

4 Conclusion

In this report, Zn-doped α-Fe_2O_3nanocomposite is synthesized through a thermal decomposition method and then applied for the photocatalytic degradation of methylene blue (MB) dye. The as-synthesized catalyst was characterized by XRD, and it was observed that the doped Zn was well incorporated into the structure but a shift in 2θ was observed towards the high *2θ* values.SEM result showed the sphere-shaped morphology of the catalyst in the range of 27-52 nm in size. The surface area of as-synthesized Zn doped α-Fe_2O_3nanocomposite was found to be 16.569, 34.543 and 17.459 m^2/g and that for pure is 12.523 m^2/g through the BET analysis.The Zn doped α-Fe_2O_3nanocomposite was found to have an improved degradation efficiency than the catalyst when used under visible light, and it showed about 92.81% degradation of MB dye within 150 minutes. Degradation of MB dye was studied by varying different parameters, such as a change in catalyst dose, pH, initial dye concentration and bubbling of O_2. Then the reusability of the catalyst was studied by performing a cyclic test, and the catalyst showed good photocatalytic activity up to seven consecutive cycles. From the results obtained, we propose Zn-doped α-Fe_2O_3nanocomposite as an efficient photocatalyst for the degradation of organic dyes, and it can be applied to other organic pollutants in the future.

5.References

[1] Zhang, Y.J.et al. (2015) Alkali-activated cements for photocatalytic degradation of organic dyes. In:*Handbook of Alkali-Activated Cements, Mortars and Concretes*. Elsevier: Amsterdam, p. 729.

[2] Zhang, Y.J. et al. (2013).*"A facile and low-cost synthesis of granulated blast furnace slag-based cementitious material coupled with Fe_2O_3catalyst for treatment of dye wastewater,"Appl. Catal*. B, Vols.138–139, pp. 9–16.

[3] Dutta, A.K., Maji, S.K.&Adhikary, B. (2014) γ-Fe_2O_3nanoparticles: An easily recoverable effective photo-catalyst for the degradation of rose bengal and methylene blue dyes in the waste-water treatment plant.*MaterialsResearchBulletin*, 49, 28–34.

[4] Li, X., Liu, Y., Zhang, C., Wen, T., Zhuang, L., Wang, X., Song, G., Chen, D., Ai, Y., Hayat, T.&Wang, X. (2018) Porous Fe_2O_3microcubes derived from metal organic frameworks for efficient elimination of organic pollutants and heavy metal ions.*ChemicalEngineeringJournal*, 336, 241–252.

[5] Guo, S.Q., Hu, Z., Zhen, M., Gu, B., Shen, B.&Dong, F. (2020) Insights for optimum cation defects in photocatalysis: A case study of hematite nanostructures.*AppliedCatalysis B*, 264, 118506.

[6] Souza, J.B. (2021)Junior Jr., et al, "On the relevance of understanding and controlling the locations of dopants in hematite photoanodes for low-cost water splitting,".*AppliedPhysicsLetters*, 119, 200501.

[7] Rasheed, R.T. et al. (2018) Preparation and characterization of hematite iron oxide (α-Fe_2O_3) by sol–gel method.*ChemicalSciencesJournal*, 9, 2.

[8] Tsege, E.L., Atabaev, T.S., Hossain, M.A., Lee, D., Kim, H.&Hwang, Y. (2016) Cu-doped flower-like hematite nanostructures for efficient water splitting applications.*Journal of Physics and Chemistry of Solids*, 98, 283–289.

[9] Meng, Q.L., Wang, Z., Chai, X., Weng, Z., Ding, R.&Dong, L. (2016) Fabrication of hematite (α-Fe_2O_3) nanoparticles using electrochemical deposition.*AppliedSurfaceScience*, 368, 303–308.

[10] Cao, Z.Q., Qin, M., Gu, Y., Jia, B., Chen, P.&Qu, X. (2016) Synthesis and characterization of Sn-doped hematite as visible light photocatalyst.*MaterialsResearchBulletin*, 77, 41–47.

[11] Mahmoodi, N.M. (2013) Photocatalytic degradation of dyes using carbon nanotube and titania nanoparticle.*Water, Air, and Soil Pollution*, 224, 1612.

[12] Oveisi, M., Mahmoodi, N.M.&Asli, M.A. (2019) Facile and green synthesis of metal–organic framework/inorganic nanofiber using electrospinning for recyclable visible-light photocatalysis.*Journal of CleanerProduction*, 222, 669–684.

[13] Alagiri, M.&Hamid, S.B.A. (2015) Sol–gel synthesis of α-Fe_2O_3nanoparticles and its photocatalytic application.*Journal of Sol-Gel Science and Technology*, 74, 783–789.

[14] Sarkar, D., Mandal, M.&Mandal, K. (2013) Design and synthesis of high performance multifunctional ultrathin hematite nanoribbons.*ACS AppliedMaterials and Interfaces*, 5, 11995–12004.

[15] Maji, S.K., Mukherjee, N., Mondal, A.&Adhikary, B. (2012) Synthesis, characterization and photocatalytic activity of α-Fe_2O_3nanoparticles.*Polyhedron*, 33, 145–149.

[16] Valenzuela, M.A., Bosch, P., Jiménez-Becerrill, J., Quiroz, O.&Páez, A.I. (2002) Preparation, characterization and photocatalytic activity of ZnO, Fe_2O_3 and $ZnFe_2O_4$.*Journal of Photochemistry and Photobiology A*, 148, 177–182.

[17] Sene Jeosadeque, J.et al. (2003).*Journal of PhysicalChemistry. Part B*, 107, 1597.

[18] Chiang, K., Amal, R.&Tran, T. (2002) Photocatalytic degradation of cyanide using titanium dioxide modified with copper oxide.*Advances in EnvironmentalResearch*, 6, 471–485.

[19] Sadeghi, M., Liu, W., Zhang, T., Stavropoulos, P.&Levy, B. (1996) Role of photoinducedchargecarrierseparationdistance in heterogeneousphotocatalysis: Oxidative degradation of CH_3OHvapor in contact with Pt/TiO_2 and CofumedTiO_2−Fe_2O_3.*Journal of Physical Chemistry*, 100, 19466–19474.

[20] Ho, W., Yu, J.C., Lin, J., Yu, J.&Li, P. (2004) Preparation and photocatalytic behavior of MoS2 and WS2 nanocluster sensitized TiO_2.*Langmuir*, 20, 5865–5869.

[21] Serpone, N. (1995) Photochemphotobiol.*Annali di Chimica*, 85, 247.

[22] Villasenor, J.et al. (1998).*J Chem Technol Biotechnol~72 : 105*,Vol. 13.

[23[Pal, B.&Sharon, M. (2002) Enhanced photocatalytic activity of highly porous ZnO thin films prepared by sol–gel process.*MaterialsChemistry and Physics*, 76, 82–87.

[24] Ding, Z., Lu, G.Q.&Greenfield, P.F. (2000) Role of the crystallitephase of TiO_2 in heterogeneousphotocatalysis for phenoloxidation in water.*Journal of Physical Chemistry B*, 104, 4815–4820.

[25] Lalithambika, K.C.et al. (2017).*Journal of MaterialsScience: Materials in Electronics*, 282062.

[26] Sherman, D.M. (2005) Electronic structures of iron (III) and manganese (IV) (hydr) oxide minerals: Thermodynamics of photochemical reductive dissolution in aquatic environments.*Geochimica et Cosmochimica Acta*, 69, 3249–3255.

[27] Marathe, Y.V., Ramanna, M.M.V. &Shrivastava, V.S.(2013)Synthesis and characterization of nanocrystalline CdS thin films grown by chemical bath deposition at different molarities for removal of methylene blue. *Desalination and Water Treatment*,51, 5813–5820.